ORIGINAL ARTICLE

Anti-tyrosinase and Anti-butyrylcholinesterase Quinolines-Based Coumarin Derivatives: Synthesis and Insights from Molecular Docking Studies

Marwa Gardelly[1] · Belsem Trimech[1] · Mabrouk Horchani[1] · Mansour Znati[1] · Hichem Ben Jannet[1] · Anis Romdhane[1]

Abstract

In this work, a series of anti-tyrosinase and anti-butyrylcholinesterase coumarin derivatives **4a–f** and **5a–f** were synthesized starting from 4-hydroxycoumarin. The condensation of 2-(arylimin)-4-hydroxycoumarins **3a–f** with dimethylformamide dimethyl acetal (DMF-DMA), used as a key reaction, afforded the precursors **4a–f**, whose acid treatment led to the formation of **5a–f**. These prepared heterocycles were characterized by spectroscopic means including ^{1}H-NMR, ^{13}C-NMR, and DCI-HRMS. Their anti-tyrosinase and anti-butyrylcholinesterase activities have been evaluated in vitro and some of them exhibited promising activity supported by the molecular docking analysis to estimate possible interactions between these compounds and active sites of both proteins tyrosinase (PDB: 2Y9W) and butyrylcholinesterase (PDB: 4TPK).

Keywords Quinoline · Coumarin · Bioactivity · Molecular docking · SAR

1 Introduction

Alzheimer's disease (AD) is a neurodegenerative disorder characterized by memory loss, behavioral abnormalities, and cognitive impairments [1]. Generally, individuals with this type of neurological disorder are elderly. The ultimate cause of memory deterioration is acetylcholine and butyrylcholine deficiency [2] in the parts of the central nervous system that mediate learning and memory functions. Many therapeutic approaches have been taken in an attempt to discover agents to treat and prevent AD [3]. Despite the development of therapies, treatment is still unsatisfactory, because of the limited efficiency of BChE inhibitors, including Tacrine [4, 5], Rivastigmine [6], and Galanthamine [7]. Nitrogen heterocyclic compounds, such as quinoline derivatives, can act as effective anticholinesterase agents [8], and may substantially improve AD symptoms [9–11]. Recently, many reports covering the development in quinoline synthesis have been published [12–15]. Quinolines, such as chloroquinine and quinine salicylate were also identified as potent inhibitors of tyrosinase [16]. The latter is a key enzyme involved in melanin biosynthesis, which is responsible for skin pigmentation [17] and plays an important role in protection against UV radiation. Many studies have shown that pigmentation disorders due to high levels of melanin can cause serious dermatological damages [18]. Skin damage is a major reason behind restricted usage of certain pharmaceuticals.

Previous research revealed that 3-substituted coumarin derivatives are very attractive scaffolds for the development of therapeutic compounds [19–22]. In addition, their anticholinesterase and anti-Alzheimer abilities are well-known [23]. A review of structure–activity relationships (SARs) indicated that chromone compounds possess good tyrosinase inhibitory potential due to their structural similarity to flavonoids, which combat pigment disorders [24].

Building on previous research, we decided to merge two pharmacophores: a differently substituted quinoline moiety to a coumarin entity, with the aim to discover original hybrid bioactive agents that inhibit tyrosinase and butyrylcholinesterase enzymes, and to discuss the structure–activity relationship (SAR) using molecular docking analysis. With this in mind, a series of substituted 4-hydroxy-3-(quinolin-2-yl)-2*H*-chromen-2-one derivatives **5a–f** were synthesized.

✉ Anis Romdhane
anis_romdhane@yahoo.fr

[1] Laboratory of Heterocyclic Chemistry, Natural Products and Reactivity, Faculty of Science of Monastir, Team: Medicinal Chemistry and Natural Products, Avenue of Environment, University of Monastir, 5019 Monastir, Tunisia

2 Experimental Section

DCI-HRMS (Desorption Chemical Ionization-High Resolution Mass Spectrometry) has been run in a GCT Premier Mass Spectrometer (Waters). ^{1}H (300 MHz) and ^{13}C (75 MHz) NMR spectra have been recorded on a Bruker AM-300 spectrometer, using CDCl$_3$ or DMSO-d_6 as solvent and none deuterated residual solvent as internal standard. Chemicals shifts (δ) are given in parts per million (ppm) and coupling constants (J) in Hertz. Melting points have been determined on a Büchi 510 apparatus using capillary tubes and are uncorrected.

3 Chemistry

3.1 General Procedure for the Synthesis of Compound 2

4-hydroxy-2*H*-chromen2-one (**1**, 4 g, 24.8 mmol) was dissolved in anhydride acetic (15 mL) and pyridine (5 mL) at room temperature. The resulted solution was brought to reflux temperature for 45 min. After cooling, the reaction crude was precipitated and collected by filtration after several washing with distilled water. The recuperated yellow solid was then recrystallized from ethanol yielding compound **2** as white crystals.

3.2 Spectral Data of Compound 2

3.2.1 3-Acetyl-4-Hydroxy-2*H*-Chromen-2-One (2)

Yield: 95%, MP: 135–137 °C; ^{1}H NMR (300 MHz, CDCl$_3$, δ): 2.78 (s, 3H, CH$_3$), 7.30 (dd, 1H, H-8, $J=8.3$ and 0.9 Hz), 7.35 (td, 1H, H-6, $J=7.6$ and 0.9 Hz,), 7.70 (td, 1H, H-7, $J=8.3$ and 1.5 Hz), 8.05 (dd, 1H, H-5, $J=7.6$ and 1.5 Hz), 17.70 (s, 1H, OH). ^{13}C NMR (75 MHz, CDCl$_3$, δ): 30.2 (CH$_3$), 101.93 (C-3), 115.2 (C-4a), 117.3 (C-8), 125.3 (C-5), 125.7 (C-6), 134.2 (C-7), 154.6 (C-8a), 159.7 (C-2), 178.4 (C-4), 205.97 (CO).

3.3 General Procedure for the Synthesis of Compounds 4a–f and 5a–f

Five hundred milligrams (0.002 mol) of 3-acetyl-4-hydroxycoumarin **2** and 227 mg (0.002 mol) of mono-substituted anilines were added to a 100 mL flask in 50 mL of ethanol. After 2 h of reflux, imines **3** were formed; they were filtered and washed with ethanol then treated with 2 eq. of dimethylformamide dimethyl acetal (DMF-DMA) (0.3 mL) in toluene (5 mL) for 10 min to form the enaminic intermediate

4 [25, 26]. The reaction was visualized using thin-layer chromatography (Elution System: EtOAc) showing the disappearance of the starting material and the appearance the major polar product. After evaporation of toluene, intermediates **4a–f** (obtained by precipitation), were brought to reflux in 5 mL of acetic acid for 1 h. The reaction crude was then precipitated in distilled water and collected by filtration to afford compounds **5a–f** (See supplementary materials for spectral data of compounds **4a–f** and **5a–f**).

3.4 Spectral Data of Compounds 4a–f and 5a–f

3-((1*E*,2*E*)-3-(dimethylamino)-1-(phenylimino)allyl)-4-hydroxy-2*H*-chromen-2-one **(4a)** Yield: 53%, MP: 200–202 °C, ^{1}H NMR (300 MHz, CDCl$_3$, δ): 2.48 (s, 6H, N(CH$_3$)$_2$), 5.78 (d, 1H, H-3′, $J=12$ Hz), 7.04 (d, 2H, H-2″,6″, $J=6$ Hz), 7.08 (m, 3H, H-4″,6,8), 7.19 (m, 3H, H-3″,5″,7), 7.34 (m, 1H, H-5), 7.94 (d, 1H, H-4′, $J=12$ Hz), 12.77 (s, 1H, OH); ^{13}C NMR (75 MHz, CDCl$_3$, δ): 42.6 (N(CH$_3$)$_2$), 88.2 (C-3), 93.0 (C-3′), 115.6 (C-4a), 116.4 (C-8), 121.0 (C-5), 122.5 (C-2″,6″), 125.2 (C-6), 126.0 (C-4″), 129.0 (C-3″,5″), 131.9 (C-7), 148.5 (C-2′), 150.2 (C-8a), 160.7 (C-2), 163.0 (C-4′), 168.3 (C-4). DCI-HRMS [M + H]$^+$ calcd. for (C$_{20}$H$_{19}$N$_2$O$_3$)$^+$: 335.1395, found 335.1405.

3.4.1 3-((1*E*,2*E*)-1-((4-Chlorophenyl)imino)-3-(Dimethylamino)allyl)-4-Hydroxy-2*H*-cChromen-2-One (4b)

Yield: 63%, MP: 202–204 °C, ^{1}H NMR (300 MHz, CDCl$_3$, δ): 2.97 (s, 6H, N(CH$_3$)$_2$), 5.74 (d, 1H, H-3′, $J=12$ Hz), 7.05 (d, 2H, H-2″,6″, $J=6$ Hz), 7.15 (td, 1H, H-7, $J=6;0.9$ Hz), 7.20 (m, 2H, H-6,8), 7.34 (d, 2H, H-3″,5″, $J=6$ Hz), 7.39 (d, 1H, H-4′, $J=12$ Hz), 8.00 (d, 1H, H-5, $J=9$ Hz), 12.65 (s, 1H, OH); ^{13}C NMR (75 MHz, CDCl$_3$, δ): 43.3 (N(CH$_3$)$_2$), 88.5 (C-3), 94.0 (C-3′), 115.2 (C-4a), 116.0 (C-8), 120.0 (C-5), 122.1 (C-2″,6″), 122.6 (C-6), 125.7 (C-7), 129.1 (C-3″,5″), 131.9 (C-4″), 147.7 (C-1″), 148.5 (C-2′), 151.1 (C-8a), 160.5 (C-2), 162.9 (C-4′), 167.9 (C-4). DCI-HRMS [M + H]$^+$ calcd. for (C$_{20}$H$_{18}$ClN$_2$O$_3$)$^+$: 369.1006, found 369.1017.

3.4.2 3-((1*E*,2*E*)-3-(Dimethylamino)-1-(p-Tolylimino)allyl)-4-Hydroxy-2*H*-Chromen-2-One (4c)

Yield: 60%, MP: 200–202 °C, ^{1}H NMR (300 MHz, CDCl$_3$, δ): 2.34 (s, 3H, CH$_3$), 2.87 (s, ^{2}&a7.30 (m, 2H, H-6,8), 7.41 (d, 2H, H-3″,5″, $J=6$ Hz) 8.02 (d, 1H, H-4′, $J=12$ Hz), 8.04 (d, 1H, H-5, $J=9$ Hz), 12.42 (s, 1H, OH); ^{13}C NMR (75 MHz, CDCl$_3$, δ): 20.7 (CH$_3$), 43.0 (N(CH$_3$)$_2$), 88.5 (C-3), 92.0 (C-3′), 115.6 (C-4a), 116.0 (C-8), 120.9 (C-5), (121.7) (C-2″,6″), 125.1 (C-6), 129.4 (C-3″,5″), 128.7 (C-7),

134.8 (C-4″), 146.4 (C-1″), 147.0 (C-2′), 151.0 (C-8a), 159.7 (C-2), 162.5 (C-4′), 168.4 (C-4). DCI-HRMS $[M+H]^+$ calcd. for $(C_{21}H_{21}N_2O_3)^+$: 349.1552, found 349.1564.

3.4.3 3-((1*E*,2*E*)-3-(Dimethylamino)-1-((4-Methoxyphenyl) imino)allyl)-4-Hydroxy-2*H* Chromen-2-One (4d)

Yield: 57%, MP: 200–202 °C, ^{1}H NMR (300 MHz, CDCl$_3$, δ): 2.97 (s, 6H, N(CH$_3$)$_2$), 3.78 (s, 3H, OCH$_3$), 5.58 (d, 1H, H-3′, *J* = 12 Hz), 6.84 (d, 2H, H-3″,5″, *J* = 9 Hz), 7.03 (d, 2H, H-2″,6″, *J* = 9 Hz), 7.11 (m, 2H, H-6,8), 7.30 (m, 2H, H-4′,7), 7.96 (d, 1H, H-5, *J* = 9 Hz), 12.20 (s, 1H, OH); ^{13}C NMR (75 MHz, CDCl$_3$, δ): 40.9 (N(CH$_3$)$_2$), 54.9 (OCH$_3$), 88.1 (C-3), 93.7 (C-3′), 114.7 (C-4a), 115.6 (C-3″,5″), 116.0 (C-8), 121.0 (C-5), 122.3 (C-2″,6″), 123.1 (C-6), 131.4 (C-7), 141.6 (C-1″), 148.7 (C-2′), 152.2 (C-8a), 160.1 (C-4″), 160.8 (C-2), 162.7 (C-4′), 167.5 (C-4). DCI-HRMS $[M+H]^+$ calcd. for $(C_{21}H_{21}N_2O_4)^+$: 368.1308, found 368.1319.

3.4.4 3-((1*E*,2*E*)-3-(Dimethylamino)-1-((4-Ethoxyphenyl) imino)allyl)-4-Hydroxy-2*H*-Chromen-2-One (4e)

Yield: 61%, MP: 200–202 °C, ^{1}H NMR (300 MHz, CDCl$_3$, δ): 1.22 (s, 3H, CH$_3$-(a)), 2.62 (q, 2H, CH$_2$-(b), *J* = 7.5 Hz), 2.92 (s, 6H, N(CH$_3$)$_2$), 5.76 (d, 1H, H-3′, *J* = 12 Hz), 7.10 (d, 2H, H-2″,6″, *J* = 9 Hz), 7.18 (d, 2H, H-3″,5″, *J* = 9 Hz), 7.23 (m, 2H, H-6,8), 7.34 (m, 2H, H-4′,7), 8.02 (d, 1H, H-5, *J* = 9 Hz), 12.40 (s, 1H, OH); ^{13}C NMR (75 MHz, CDCl$_3$, δ): 15.0 (CH$_3$-(a)), 42.9 (N(CH$_3$)$_2$), 64.2 (CH$_2$-(b)), 88.2 (C-3), 92.0 (C-3′), 115.6 (C-4a), 116.5 (8), 121.1 (C-5), 117.6 (C-2″,C-6″), 121.3 (C-3″,5″), 122.5 (C-6), 128.1 (7), 142.4 (C-1″), 147.9 (C-2′), 152.2 (C-8a), 154.2 (C-4″), 159.9 (C-2), 163.3 (C-4′), 168.5 (C-4). DCI-HRMS $[M+H]^+$ calcd. for $(C_{22}H_{23}N_2O_4)^+$: 379.1658, found 379.1670.

3.4.5 3-((1*E*,2*E*)-1-((3-Chlorophenyl) imino)-3-(Dimethylamino)allyl)-4-Hydroxy-2*H*-Chromen-2-One (4f)

Yield: 76%, MP: 202–204 °C, ^{1}H NMR (300 MHz, CDCl$_3$, δ): 2.83 (s, 6H, N(CH$_3$)$_2$), 5.75 (d, 1H, H-3′, *J* = 12 Hz), 6.95 (d, 1H, H-6″, *J* = 9 Hz), 7.09 (m, 2H, H-6,8), 7.32 (m, 2H, H-4′,7), 7.47 (d, 1H, H-4″, *J* = 9 Hz), 7.57 (t, 1H, H-5″, *J* = 9 Hz), 7.85 (s, 1H, H-2″), 7.91 (d, 1H, H-5, *J* = 9 Hz), 12.40 (s, 1H, OH); ^{13}C NMR (75 MHz, CDCl$_3$, δ): 44.0 (N(CH$_3$)$_2$), 88.6 (C-3), 94.0 (C-3′), 115.5 (C-4a), 116.7 (C-8), 120.9 (C-6″), 122.4 (C-2″), 122.6 (C-5), 124.3 (C-6), 125.9 (C-4″), 129.9 (C-7), 131.7 (C-5″), 134.4 (C-3″), 148.0 (C-2′), 152.9 (C-1″), 153.2 (C-8a), 162.0 (C-2), 163.1 (C-4′), 167.5 (C-4). DCI-HRMS $[M+H]^+$ calcd. for $(C_{20}H_{18}ClN_2O_3)^+$: 369.1006, found 369.1011.

3.4.6 4-Hydroxy-3-(Quinolin-2-yl)-2*H*-Chromen-2-One (5a)

Yield: 52%, MP: 300–302 °C, ^{1}H NMR (300 MHz, DMSO-d_6, δ): 7.17 (m, 1H, H-6), 7.22 (m, 1H, H-8), 7.34 (m, 4H, H-5,7,5′,3′), 7.71 (m, 1H, H-6′), 7.81 (s, 1H, H-7′), 7.96 (d, 1H, H-4′, *J* = 6 Hz), 8.68 (d, 1H, H-8′, *J* = 6 Hz), 11.37 (s, 1H, OH); ^{13}C NMR (75 MHz, DMSO-d_6, δ): 97.6 (C-3), 116.4 (C-8), 117.4 (C-4a), 119.8 (C-3′), 123.3 (C-5), 123.8 (C-6), 125.6 (C-6′), 128.3 (C-4′a), 128.7 (C-5′), 130.4 (C-7), 131.7 (C-8′), 132.1 (C-7′), 135.4 (C-4′), 146.7 (C-8′a), 152.5 (C-8a), 159.1 (C-2′), 161.9 (C-2), 166.4 (C-4). DCI-HRMS $[M+H]^+$ calcd. for $(C_{18}H_{12}NO_3)^+$: 290.0817, found 290.0825.

3.4.7 3-(6-Chloroquinolin-2-yl)-4-Hydroxy-2*H*-Chromen-2-One (5b)

Yield: 71%, MP: 300–302 °C, ^{1}H NMR (300 MHz, DMSO-d_6, δ): 7.33 (m, 6H, H-3′,5′,5,6,7,8), 7.71 (s, 1H, H-7′), 7.99 (d, 1H, H-4′, *J* = 6 Hz), 8.06 (d, 1H, H-8′, *J* = 9 Hz), 11.37 (s, 1H, OH); ^{13}C NMR (75 MHz, DMSO-d_6, δ): 97.6 (C-3), 116.4 (C-8), 117.4 (C-4a), 119.8 (C-3′), 123.3 (C-5), 123.7 (C-5′), 125.1 (C-6), 128.0 (C-7), 128.7 (C-4′a), 130.2 (C-8′), 131.5 (C-7′), 132.4 (C-6′), 135.8 (C-4′), 146.0 (C-8′a), 151.8 (C-8a), 159.5 (C-2′), 161.7 (C-2), 166.7 (C-4). DCI-HRMS $[M+H]^+$ calcd. for $(C_{18}H_{11}ClNO_3)^+$: 324.0427, found 324.0438.

3.4.8 4-Hydroxy-3-(6-Methylquinolin-2-yl)-2*H*-Chromen-2-One (5c)

Yield: 45%, MP: 260–262 °C, ^{1}H NMR (300 MHz, DMSO-d_6, δ): 2.30 (s, 3H, CH$_3$), 6.89 (m, 3H, H-6,8,8′), 7.19 (m, 3H, H-7,3′,6′), 7.54 (d, 1H, H-4′, *J* = 6 Hz), 7.98 (d, 1H, H-7′, *J* = 6 Hz), 11.14 (s, 1H, OH); ^{13}C NMR (75 MHz, DMSO-d_6, δ): 21.4 (CH$_3$), 95.0 (C-3), 114.0 (C-8), 116.6 (C-4a), 117.8 (C-3′), 123.9 (C-5), 125.1 (C-5′), 128.7 (C-4′a), 128.9 (C-6), 129.3 (C-8′), 129.7 (C-7), 131.7 (C-7′), 134.7 (C-4′), 135.7 (C-6′), 146.0 (C-8′a), 152.5 (C-8a), 154.1 (C-2′), 160.0 (C-2), 168.4 (C-4). DCI-HRMS $[M+H]^+$ calcd. for $(C_{19}H_{14}NO_3)^+$: 304.0974, found 304.0988.

3.4.9 4-Hydroxy-3-(6-Methoxyquinolin-2-yl)-2*H*-Chromen-2-One (5d)

Yield: 75%, MP: 260–262 °C, ^{1}H NMR (300 MHz, DMSO-d_6, δ): 3.78 (s, 3H, OCH$_3$), 6.97 (m, 2H, H-5′,7′), 7.19 (d, 1H, H-3′, *J* = 6 Hz), 7.29 (m, 3H, H-6,7,8), 7.68 (t, 1H, H-5, *J* = 6 Hz), 7.97 (d, 1H, H-8′, *J* = 6 Hz), 8.57 (d, 1H, H-4′, *J* = 6 Hz), 11.24 (s, 1H, OH); ^{13}C NMR (75 MHz, DMSO-d_6, δ): 55.3 (OCH$_3$), 95.3 (C-3), 104.9 (C-5′), 115.9 (C-8), 117.1 (C-4a), 119.0 (C-3′), 121.1 (C-7′), 123.0 (C-5), 125.4 (C-6), 127.1 (C-7), 128.9 (C-4′a), 131.5 (C-8′), 134.7 (C-4′),

143.5 (C-8′a), 153.3 (C-8a), 156.7 (C-6′), 157.4 (C-2′), 160.7 (C-2), 168.5 (C-4). DCI-HRMS [M+H]$^+$ calcd. for $(C_{19}H_{14}NO_4)^+$: 320.0923, found 320.0927.

3.4.10 3-(6-Ethoxyquinolin-2-yl)-4-Hy-droxy-2*H*-Chromen-2-One (5e)

Yield: 48%, MP: 270–272 °C, ^{1}H NMR (300 MHz, DMSO-d_6, δ): 1.11 (t, 3H, CH$_3$-(a), $J = 2.7$ Hz), 2.58 (q, 2H, CH$_2$ (b), $J = 6$ Hz), 7.26 (m, 6H, H-5,6,7,8,6′,8′), 7.46 (d, 1H, H-3′, $J = 6$ Hz), 7.68 (d,1H, H-4′, $J = 6$ Hz), 8,63 (d, 1H, H-7′, $J = 6$ Hz), 11,37 (s,1H, OH); ^{13}C NMR (75 MHz, DMSO-d_6, δ): 14.5 (CH$_3$ (a)), 64.4 (CH$_2$ (b)), 95.8 (C-3), 106.1 (C-5′), 116.0 (C-8), 116.4 (C-4a), 117.5 (C-3′), 122.1 (C-7′), 124.0 (C-5), 127.3 (C-6), 129.0 (C-7), 129.7 (C-4′a), 130.5 (C-8′), 134.7 (C-4′), 144.9 (C-8′a), 152.0 (C-8a), 153.4 (C-2′), 157.4 (C-6′), 160.9 (C-2), 166.4 (C-4). DCI-HRMS [M+H]$^+$ calcd. for $(C_{20}H_{16}NO_4)^+$: 334.1079, found 334.1084.

3.4.11 3-(7-Chloroquinolin-2-yl)-4-Hy-droxy-2*H*-Chromen-2-One (5f)

Yield: 63%, MP: 280–282 °C, ^{1}H NMR (300 MHz, DMSO-d_6, δ): 7.14 (d, 1H, H-3′, $J = 6.0$ Hz),7,22 (m, 4H, H-5,6,8,8′), 7.63 (t, 1H, H-7, $J = 6.0$ Hz), 7,95 (d, 1H, H-5′, $J = 6.0$ Hz), 8.59 (d, 1H, H-4′, $J = 6.0$ Hz), 11,18 (s, 1H, OH); ^{13}C NMR (75 MHz, DMSO-d_6, δ): 97.1 (C-3), 116.4 (C-8), 117.0 (C-4a), 118.4 (C-3′), 123.3 (C-5), 124.4 (C-5′), 125.3 (C-6), 128.0 (C-7), 127.4 (C-4′a), 127.9 (C-6′), 129.3 (C-8′), 135.1 (C-7′), 136.2 (C-4′), 147.0 (C-8′a), 152.1 (C-8a), 159.8 (C-2′), 161.0 (C-2), 166.5 (C-4). DCI-HRMS [M+H]$^+$ calcd. for $(C_{18}H_{11}ClNO_3)^+$: 324.0427, found 324.0435.

4 Biological

4.1 Anti-tyrosinase Activity

The effect of inhibitor on mushroom tyrosinase was measured using L-tyrosine (1 mM) as the substrate. Hydroquinone (1 mM) was chosen as tyrosinase inhibitor. Both substrate and inhibitor were prepared in 0.1 M phosphate buffer pH 6.5. Inhibition of tyrosinase activity was tested in a reaction mixture (4 mL) containing 1.960 mL phosphate buffer, 2 mL L-tyrosine (1 mM), 20 µL mushroom tyrosinase and 20 µL hydroquinone (1 mM). The reaction was initiated by addition of enzyme to the solution of substrate and inhibitor. Then, the reaction cell and all solutions were both thermostated at 25 °C. Inhibition effect was determined by the diminution of the maximum quantity of dopachrome formed and the absorbance was measured spectrophotometrically at 475 nm. The inhibition percentage of tyrosinase activity was calculated as: Inhibition (%) = (A-B)/A × 100. Where A represents the optical density of the tyrosinase enzyme and B represents the optical density of the tested samples during 30 min. The assay was carried out in triplicate and Kojic acid was used as positive control agent. Sample concentration providing 50% inhibition (IC$_{50}$) was obtained plotting the inhibition percentage against sample concentrations [27].

4.2 Anti-butyrylcholinesterase Activity

Human plasma (pool plasma from samples designated for biochemical analysis) was used as a source of BChE. 100 µL of each sample were added to 100 µL of plasma and the mixture was incubated at 37 °C for 15 min. After incubation, the enzyme activity was measured by Konelab 30® UV apparatus at 405 nm. The control (plasma and distilled water) was treated in the same conditions. The assay was achieved in duplicate. Galanthamine was chosen as control positive. The anti-butyrylcholinesterase activity was calculated using the following formula: % Inhibition = [(Activity of control—Activity of sample)/Activity of control] × 100. The sample concentration providing 50% inhibition (IC$_{50}$) was determined by plotting inhibition percentages against concentrations of the sample. To evaluate temperature and incubation times effects, assays were performed by using the same procedure for the same sample, at 25 °C (fixed incubation times) and for different times at 37 °C [28].

4.3 Molecular Docking Procedure

The three-dimensional structures of PDB (PDB: 2Y9W) and PDB (PDB: 4TPK) were obtained from the RSCB protein data bank [29, 30]. Before conducting the docking procedure, the original ligands and water molecules were removed. The polar hydrogens were then added to the enzyme structure. The optimization of all the geometries of scaffolds was performed with ACD (3D viewer) software (http://www.filefacts.com/acd3d-viewer-freeware-info). Molecular docking of the studied chemical compounds **5a**, **5c**, **5d**, **5e**, and **5f** at the tropolone-binding site was performed using autodock Vina software [31]. The analysis of intermolecular interactions has been performed using Pymol Version 0.99rc6.

5 Results and Discussion

5.1 Chemistry

We used DMF-DMA as a key reagent because of its high reactivity [25, 26]. 4-Hydroxy-3-(quinolin-2-yl)-2*H*-chromen-2-one derivatives **5a–f** were synthesized through a four-step reaction (Scheme 1). The 3-acetyl-4-hydroxy-coumarin **2** obtained by acetylation of 4-hydroxycoumarin

Scheme 1 Synthesis of 4-hydroxy-3-(quinolin-2-yl)-2*H*-chromen-2-ones **5a–f**. *Reaction conditions*: (i) Acetic anhydride, pyridine, 150 °C, reflux 2 h; (ii) Aromatic amines, EtOH, 79 °C, reflux 4 h; (iii) DMF-DMA (2 eq), Toluene, 110 °C, reflux 10 min; (iv) Acetic acid, 117 °C, reflux 1 h
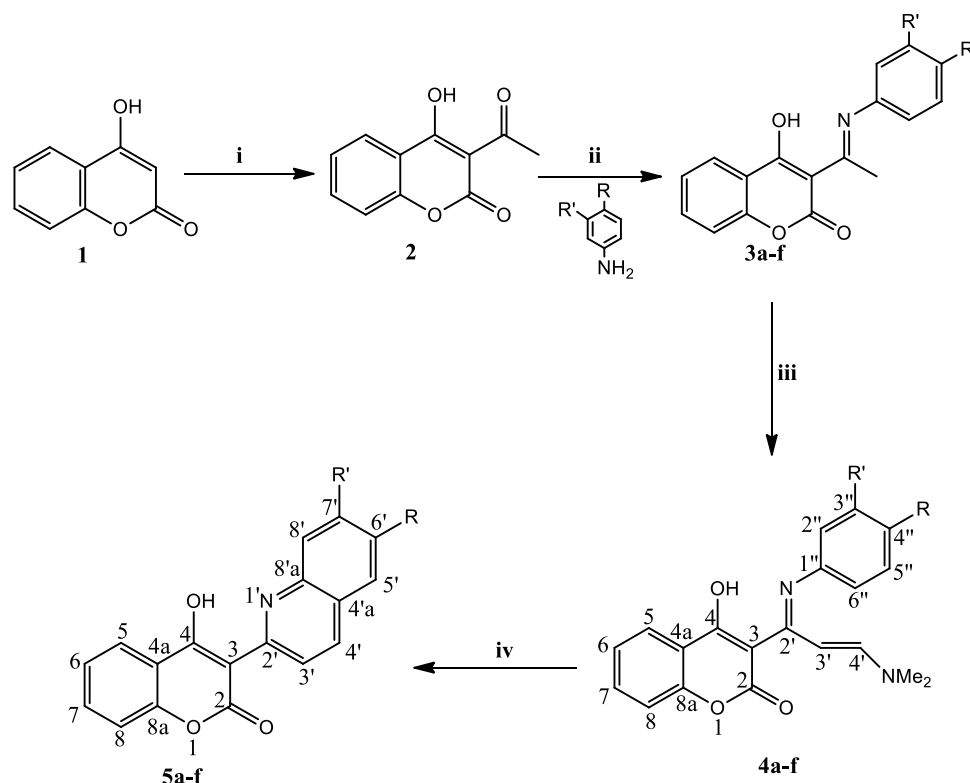
1 was condensed with a series of primary aromatic amines, in ethanol, for 4 h to afford compounds **3**. Compounds **4a–f**, prepared by treating **3** with DMF-DMA in toluene for 10 min, were heated in acetic acid for 1 h to produce the target compounds **5a–f** (Table 1).

Mechanically, the formation of compound **5** (Scheme 2) starts by the protonation of dimethyl nitrogen in intermediates **4**, the free doublet of nitrogen $N_{1'}$ being engaged in an intramolecular hydrogen bond with the OH group of the coumarin moiety. Cyclization of this intermediate was made possible by an intramolecular rearrangement similar to that of Diels–Alder reactions, thus producing the **5a–f** derivatives after aromatization and departure of an NHMe2 molecule. The structures of substituted 4-hydroxy-3-(quinolin-2-yl)-2*H*-chromen-2-one derivatives **5a–f**, were assigned on the basis of on their ^{1}H and ^{13}C NMR spectral data. The DCI-HRMS mass spectra of all the compounds were consistent with the proposed structures.
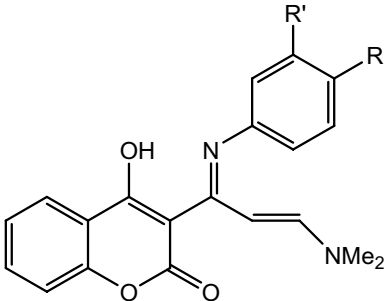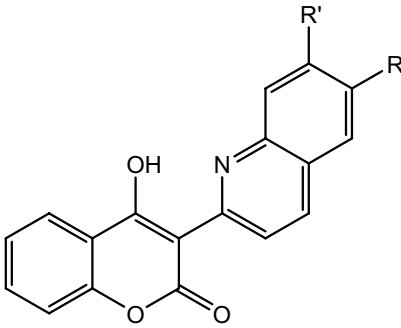
5.2 Biological

Compounds **4** and **5** were evaluated for their anti-tyrosinase and anti-butyrylcholinesterase activities.

5.2.1 Anti-tyrosinase Inhibitory

The anti-tyrosinase activity of compounds **4a–f** and **5a–f** was carried. The results clearly indicated that compounds **5a–f** were more active than their precursors **4a–f**, demonstrating the net contribution importance of the formed quinoline system, which appeared to be involved in the inhibition of tyrosinase (Table 2). Compounds **5a**, **5c**, **5e**, and **5f** were found to display remarkable tyrosinase inhibiting abilities ($IC_{50} = 17.5 \pm 1.0$, 18.3 ± 0.5, 17.9 ± 0.7 and 15.1 ± 0.8 μM, respectively) compared to the positive control kojic acid ($IC_{50} = 12.1 \pm 0.2$ μM). The compound **5f** with a chlorine atom in $C_{7'}$ position showed the highest activity. The unsubstituted quinoline **5a** displayed an important activity. This finding shows the importance of the chlorine atom in **5f** which is certainly at the origin of the improvement of this activity. On the other hand, by comparing the activity of analogues **5b** (R = Cl, R' = H) ($IC_{50} = 28.7 \pm 1.1$ μM) and **5f** (R = H, R' = Cl), we can clearly see the influence of this position on the activity. Indeed, the chlorine in the meta-position was found to be more effective in terms of anti-tyrosinase activity. The inductive and mesomeric electronic effects exerted by the chlorine atom in each position could be at the origin of this difference in activity. The compound **5c** with a methyl group at $C_{6'}$, and the unsubstituted compound **5a**, exhibited a comparable anti-tyrosinase effect, this suggests that the methyl group cannot be considered as a good candidate substituent which can improve this activity. Compound **5d** with a methoxy at $C_{6'}$ was found to be less active ($IC_{50} = 24.9 \pm 1.1$ μM) than its analog **5e** with an ethoxy group in the same position. This result shows clearly the

Table 1 Compounds **4a–f** and **5a–f**: structures and yields

Entry	Product	Main structure of compounds	R	R'	Yields (%)
1	**4a**		H	H	53

2	**4b**		Cl	H	63
3	**4c**		Me	H	60
4	**4d**		OMe	H	57
5	**4e**		OEt	H	61
6	**4f**		H	Cl	76
7	**5a**		H	H	52

|					
8	**5b**		Cl	H	71
9	**5c**		Me	H	45
10	**5d**		OMe	H	75
11	**5e**		OEt	H	48
12	**5f**		H	Cl	63

influence of the nature of the alkoxy group attached at $C_{6'}$ position on this activity.

The results described above clearly show the contribution of the quinoline fragment introduced to have this activity compared with that of the precursors **4a–f**. This finding agrees well with the literature data showing the significant activity of quinoline derivatives, such as chloroquine [16] with a chlorine atom at the same position as the more active **5f** derivative of the series **5**.

5.2.2 Anti-butyrylcholinesterase Activity

Compounds **5a–f** and their precursors **4a–f** were assessed using an anti-butyrylcholinesterase test and the IC_{50} values are indicated in Table 3. The compounds **4a–f** were found to be less active than **5a–f** ones. These results revealed the importance of cyclization, leading to the formation of quinoline, which appeared to be involved in the inhibition of BChE. The compound **5d** with a methoxy group

exhibited the highest anti-BChE effect with an IC_{50} value of 40.0 ± 0.4 μM, followed by the derivative **5f** with a chlorine atom at $C_{7'}$ ($IC_{50} = 51.0 \pm 0.5$ μM). The activity of the later compared to that of its analogue **5b** with a chlorine atom at $C_{6'}$ ($IC_{50} = 89.0 \pm 0.8$ μM) allows to notice the influence of the position of the chlorine atom on this activity. The activity of these two chlorinated derivatives **5f** and **5b** compared to that of the unsubstituted compound **5a** ($IC_{50} = 112.0 \pm 2.0$ μM), shows the importance of the chlorine atom whatever its position in improving this activity. The inductive and mesomeric electronic effects exerted by the chlorine atom in each position could explain this difference in activity. On the other hand, the compound **5d** with a methoxy group at $C_{6'}$ showed twice the activity of its analogue **5e** ($IC_{50} = 79.0 \pm 0.5$ μM) with an ethoxy group at the same position ($IC_{50} = 79.0 \pm 0.5$ μM). This showed that we may not need to extend the alkyl group of the alkoxy moiety to obtain better activity. Testing other compounds with longer alkoxy groups is necessary to provide greater support

Scheme 2 Plausible mechanism for the formation of compounds **5a–f**
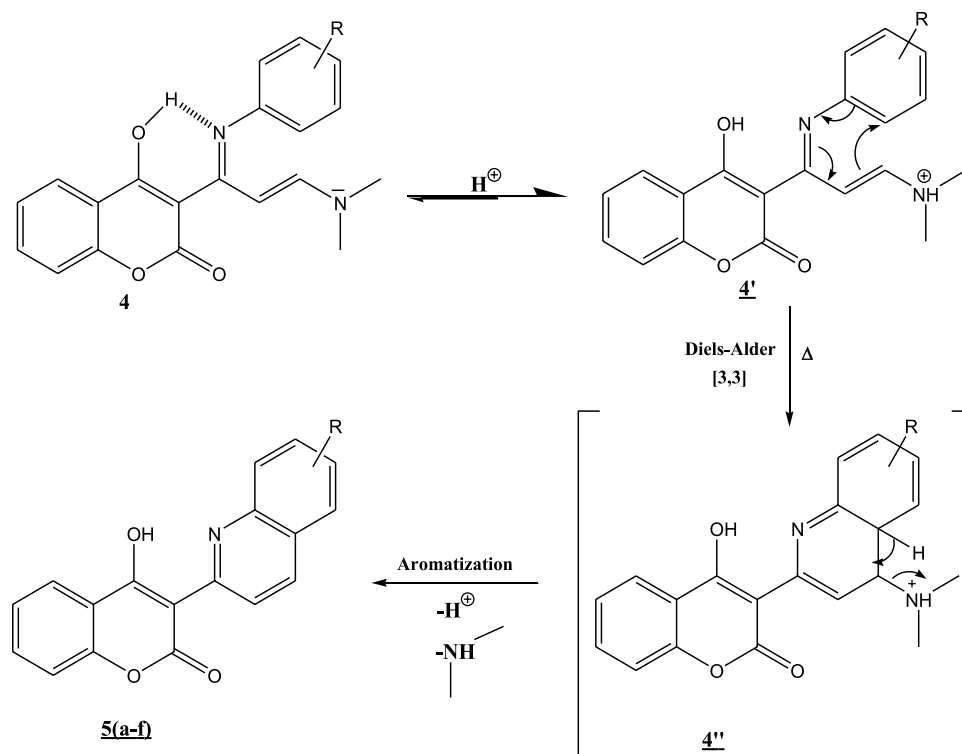
Table 2 Anti-tyrosinase activity of compounds **4a–f** and **5a–f**

Compound	IC$_{50}$ (µM)^a
4a	102.0 ± 2.0
4b	> 100
4c	> 100
4d	> 100
4e	95.2 ± 3.3
4f	81.8 ± 1.9
5a	17.5 ± 1.0
5b	28.7 ± 1.1
5c	18.3 ± 0.5
5d	24.9 ± 1.1
5e	17.9 ± 0.7
5f	15.1 ± 0.8
Kojic acid	12.1 ± 0.2

^{a}The concentration of compound that inhibits 50% of the enzyme (mean $\pm$ SD, n = 3)

Table 3 Anti-butyrylcholinesterase activity of compounds **4a–f** and **5a–f**

Compound	IC$_{50}$ (µM)^a
4a	233.0 ± 3.8
4b	154.0 ± 2.6
4c	198.0 ± 2.7
4d	144.0 ± 2.6
4e	150.0 ± 3.1
4f	167.0 ± 3.0
5a	112.0 ± 2.0
5b	89.0 ± 0.8
5c	99.0 ± 1.0
5d	40.0 ± 0.4
5e	79.0 ± 0.5
5f	51.0 ± 0.5
Galanthamine	$380 \times 10^{-3} \pm 0.002 \times 10^{-3}$

^{a}The concentration of compound that inhibits 50% of the cell proliferation (mean $\pm$ SD, n = 3)

for this conclusion. The relatively weak activity of compound **5c** with a methyl group at C$_{6'}$ (IC$_{50}$ = 99.0 ± 1.0 µM) when compared to the rest of the substituted derivatives leads to the conclusion that this methyl group is not much involved in the possible interactions between the ligand and the amino acids of the enzyme.

The contribution of the introduced quinoline moiety to the anti-BChE activity of the **5a–f** compounds is defended by the data from the literature which show that quinoline-based scaffold, once introduced into a molecule, improves its anti-BChE potential [29].

6 The Molecular Docking Studies

6.1 Molecular Docking Analysis for Anti-tyrosinase Activity (PDB: 2Y9W)

Tyrosinase (PDB code: 2Y9W) is a tetrameric protein composed of four chains (A, B, C, and D) with the sequence length of 391. This binuclear copper-containing enzyme catalyzes the conversion of monophenol (tyrosine) and o-diphenol (L-DOPA) to the corresponding o-quinone derivative [30].

Molecular modeling studies were carried out by using Autodock Vina software [31] to understand the interactions of synthesized compounds **5a–f** within the hydrophobic binding pocket of tropolone (PDB: 2Y9W), and to investigate the binding modes and binding energies (Table 4) that lead to the observed SARs and differences in IC_{50}.

The analyses of binding affinities and molecular interactions for the 4-hydroxy-3-(quinolin-2-yl)-2*H*-chromen-2-one derivatives found **5a**, **5c**, **5e**, and **5f** were the most active. As Table 4 indicates, the values of binding energy of these derivatives are higher than that of the control (kojic acid).

The SARs of the anti-tyrosinase agents in Fig. 1 support that compound **5a** exercises through its coumarinic fragment a pi sigma interaction (dark purple color) with VAL-A-248, a conventional hydrogen bond interaction (green color) with HIS-A-244 and by its quinoline fragment a pi-pi stacking (dark pink color) with PHE-A-264 and pi alkyl interaction (light pink color) with VAL-A-283. Derivative **5c** forms some hydrophobic interactions with VAL-A-248 and VAL-A-283 (pi sigma), HIS-A-259 (pi-pi shaping (dark pink color)), HIS-A-263 (pi-pi stacking), SER-A-282 (amide pi stacking (dark pink color)), ALA-A-286 (pi alkyl interaction), VAL-A-248 (alkyl interactions (light pink color)) and with HIS-A-85 (carbon hydrogen bond (grey color)) (Fig. 1). Further, compound **5e** is involved in pi alkyl interactions

Table 4 Binding affinity of promising anti-tyrosinase agents towards amino acid residuals

Binding energy (kcal/mol)					
5a	− 7.5	− 7.5	− 6.7	− 6.7	− 6.5	− 6.0
5c	− 7.4	− 7.0	− 6.9	− 6.0	− 6.0	− 5.8
5e	− 7.9	− 7.2	− 6.9	− 6.5	− 6.5	− 6.2
5f	− 8.2	− 8.0	− 7.2	− 7.2	− 6.7	− 6.4
Kojic acid	− 5.7	− 5.4	− 5.2	− 5.0	− 5.0	− 4.9

Fig. 1 Binding pose of conjugates **5a**, **5c** and **5e** in the tropolone binding cavity of PDB: 2Y9W.
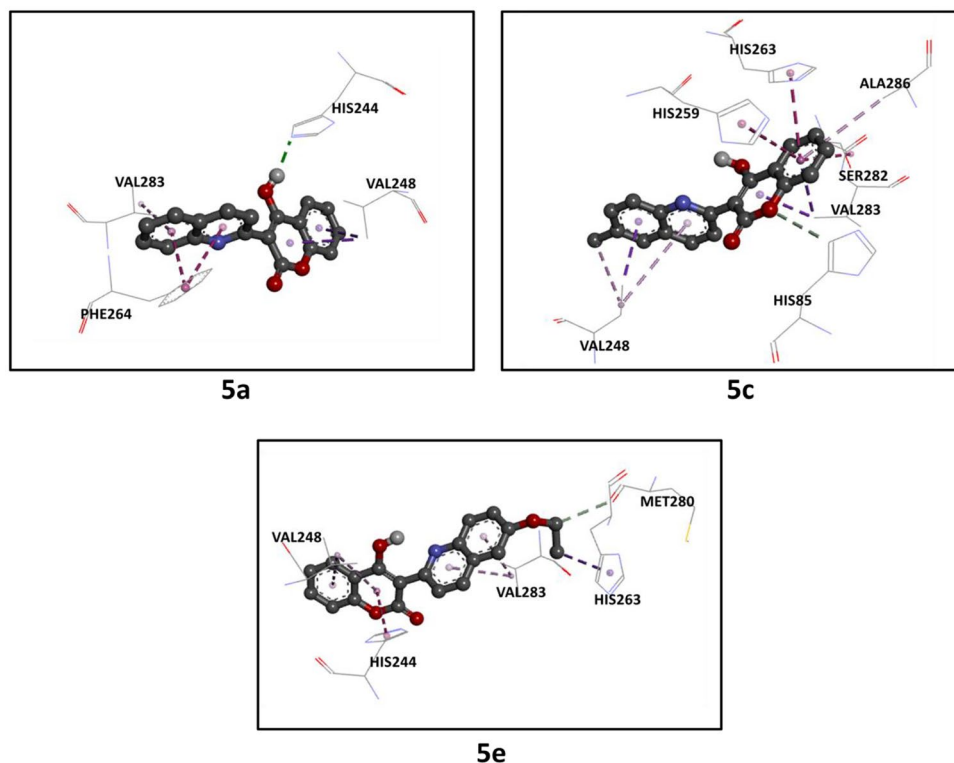
with VAL-A-248 and VAL-A-283. Besides, it displayed a pi-pi shaping with HIS-A-244, a pi sigma interaction with HIS-A-263 and carbon hydrogen bond with MET-A-280 (Fig. 1).

The most effective anti-tyrosinase agent **5f** having the lowest binding affinity (Table 4) established interactions with residues HIS-A-244, VAL-A-248, HIS-A-263 and PHE-A-264 and VAL-A-283. In details, **5f** was strongly bound by the hydroxyl functional group with HIS-A-244 in conventional hydrogen bond interactions, pi sigma interaction with VAL-A-248, pi-pi stacking with PHE-A-264, alkyl and pi alkyl interactions with HIS-A-263, PHE-A-264 and VAL-A-283 (Fig. 2).

6.2 Molecular Docking Analysis for Anti-butyrylcholinesterase Activity (PDB: 4TPK)

To understand the anticholinesterase potential of derivative **5d**, binding interactions between ligand and butyrylcholinesterase BChE (PDB: 4TPK (chain A)) were analyzed [32]. Molecular docking analysis was performed using Autodock Vina software [31]. Figure 3 showed that

hydroxycoumarin is involved in conventional hydrogen bonding (green color) by its hydroxyl functional groups with SER-A-198 and pi-pi shaping interactions (dark pink color) with TRP-A-231 and PHE-A-329 besides to pi alkyl interaction (light pink color) with LEU-A-286. Further, methoxyquinoline ring forms amide pi stacking interaction (dark pink color) with GLY-A-116, pi-pi shaping interaction with TRP-A-82, pi donor hydrogen bond with THR-A-120 and carbon hydrogen bond (grey color) with GLN-A-67.

7 Conclusion

In summary, we develop here a simple and easy method to synthesize heterocyclic compounds in a short time and with good yields. This was achieved by including quinoline and 4-hydroxycoumarin moieties in their structure, using DMF-DMA as the main reagent. We examined the anti-tyrosinase and anti-butyrylcholinesterase activities of these prepared heterocycles and some of them exhibited interesting anti-tyrosinase and butyrylcholinesterase activities. Molecular docking analyses lead to the conclusion that the quinoline

Fig. 2 Docking pose of compound **5f** (most effective anti-tyrosinase agent) in the active site of tropolone hydrophobic cavity of PDB: 2Y9X
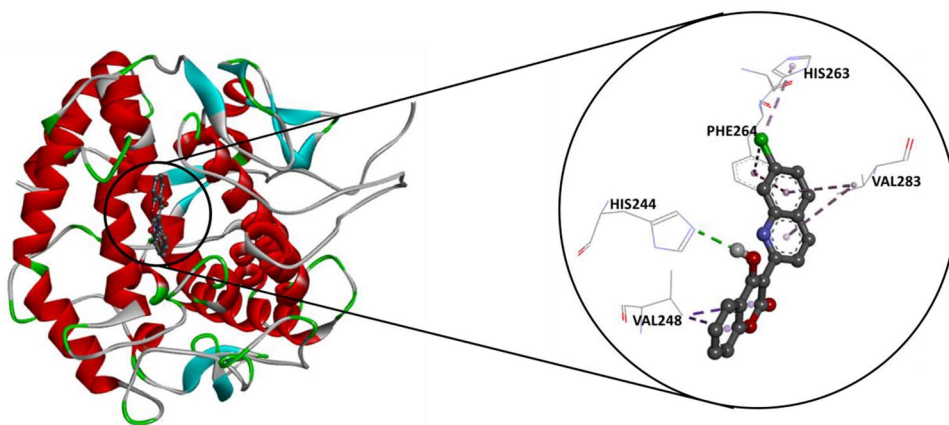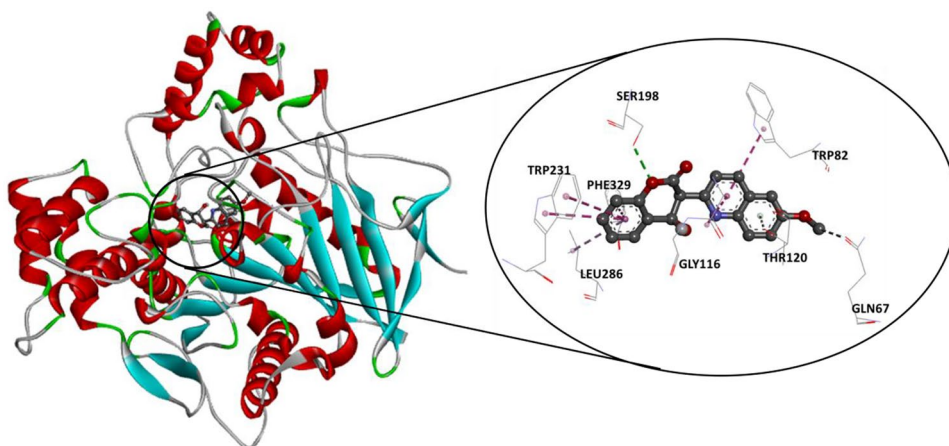

Fig. 3 Docking pose of compound **5d** in the active site of BChE (PDB: 4TPK)

moiety is essential for the build-up and improvement of anti-tyrosinase and anti-butyrylcholinesterase activities of conjugates **5a**–**f**. In silico *SAR* studies were found in good agreement with biological evaluation showing that the nature of the substitute on the quinoline ring is essential to give significant binding interaction with amino acids of enzymes. The chlorine atom appears to be in favor with the activities studied. The diversification of its position and its number merit further study.

Compliance with Ethical Standards

Conflict of interest The authors declare that they no conflict of interest.

References

1. DeTure MA, Dickson DW (2019) The neuropathological diagnosis of Alzheimer's disease. Mol Neurodegeneration 14:32–49. https://doi.org/10.1186/s13024-019-0333-5
2. Stanciu GD, Luca A, Rusu RN, Bild V, Chiriac SIB, Solcan C, Bild W, Ababei DC (2020) Alzheimer's disease pharmacotherapy in relation to cholinergic system involvement. Biomolecules 10:40–59. https://doi.org/10.3390/biom10010040
3. BrintonR D, YamazakiRS, (1998) Advances and challenges in the prevention and treatment of Alzheimer's disease. Pharm Res 15:386–389
4. Pourabdi L, Khoobi M, Nadri H, Moradi A, Moghadam FH, Emami S, Mojtahedi MM, Haririan I, Forootanfar H, Ameri A, Foroumadi A, Shafiee A (2016) Synthesis and structure activity relationship study of tacrine-based pyrano [2.3-*c*]pyrazoles targeting AchE/BuchEand 15-LOX. Eur J Med Chem 123:298–308. https://doi.org/10.1016/j.ejmech.2016.07.043
5. Benchekroun M, Ismaili L, Pudlo M, Luzet V, Gharbi T, Refouvelet B, Marco-Contelles J (2015) Donepezil-ferulic acid hybrids as anti-Alzheimer drugs. Future Med Chem 7:15–21. https://doi.org/10.4155/fmc.14.148
6. Simon A, Amaro MI, Healy AM, Cabral LM, de Sousa VP (2016) Comparative evaluation of rivastigmine permeation from a transdermal system in the Franz cell using synthetic membrane and pig ear skin with in vivo-in vitro correlation. Int J Pharm 512:234–241. https://doi.org/10.1016/j.ijpharm.2016.08.052
7. Sanli N, Bulduk I, Ozkurt H, Şanli S, Ozkan SA (2016) Development and validation of capillary zone electrophoretic method for rapid and sensitive determination of galanthamine: application in plants and pharmaceuticals. J Pharm Biomed Anal 131:188–194. https://doi.org/10.1016/j.jpba.2016.08.026
8. Zajdel P, Marciniec K, Maślankiewicz A, Grychowska K, Satała G, Duszyńska B, Lenda T, Siwek A, Nowak G, Partyka A, Wróbel D, Jastrzębska-Więsek M, Bojarski AJ, Wesołowska A, Pawłowski M (2013) Antidepressant and antipsychotic activity of new quinolone and isoquinoline-sulfonamide analogs of aripiprazole targeting serotonin 5-HT$_1$A/5-HT$_2$A/5-HT$_7$ and dopamine D$_2$/D$_3$ receptors. Eur J Med Chem 60:42–50. https://doi.org/10.1016/j.ejmech.2012.11.042
9. Rampa A, Bisi A, Belluti F, Gobbi S, Valenti P, Andrisano V, Cavrini V, Cavalli A, Recanatini M (2000) Acetylcholinesterase inhibitors for potential use in Alzheimer's disease: molecular modeling, synthesis and kinetic evaluation of 11H-indeno-[1,2-*b*]-quinolin-10-ylamine derivatives. Bioorg Med Chem Lett 8:497–506. https://doi.org/10.1016/s0968-0896(99)00306-5
10. Zhong W, Liu H, Kaller MR, Henley C, Magal E, Nguyen T, Osslund TD, Powers D, Rzasa RM, Wang HL, Wang W, Xiong X, Zhang J, Norman MH (2007) Synthesis and design of quinolin-2(1H)-one derivatives as potent CDK5 inhibitors. Bioorg Med Chem Lett 17:5384–5389. https://doi.org/10.1016/j.bmcl.2007.07.045
11. Oset-Gasque MJ, González MP, Pérez-Peña J, García-Font N, Romero A, del Pino J, Ramos E, Hadjipavlou-Litina D, Soriano E, Chioua M, Samadi A, Raghuvanshi DS, Singh KN, Marco-Contelles J (2014) Toxicological and pharmacological evaluation antioxidant, ADMET and molecular modelingof selected racemic chromenotacrines 11amino-12-aryl-8,9,10,12-tetrahydro-7H-chromeno[2,3-b]quinolin-3-ols for the potential prevention and treatment of Alzheimer's disease. Eur J Med Chem 74:491–501. https://doi.org/10.1016/j.ejmech.2013.12.021
12. Murru S, Gough BM, Srivastava RS (2014) Synthesis of substituted quinolines via allylic amination and intermolecular Heck coupling. Org Biomol Chem 12:9133–9138
13. Selig P, Raven W (2014) A convenient alenoate-based synthesis of 2-quinolin-2-one malonates and β-ketoesters. Org Lett 16:5192–5195. https://doi.org/10.1021/ol502554e
14. Zhou S, Ren J, Liu M, Ren L, Liu Y, Gong P (2014) Design, synthesis and pharmacological evaluation of 6,7-disubstituted-4-phenoxyquinoline derivatives as potential antitumor agents. Bioorg Chem 57:30–42. https://doi.org/10.1016/j.bioorg.2014.07.011
15. Xuan DD (2019) Recent progress in the synthesis of quinolines 16:671–708. https://doi.org/10.2174/1570179416666190719112423
16. Ni-Komatsu L, Tong C, Chen G, Brindzei N, Orlow SJ (2008) Identification of quinolines that inhibit melanogenesis by altering tyrosinase family trafficking. Mol Pharmacol 74:1576–1586. https://doi.org/10.1124/mol.108.050633
17. Lin JY, Fisher DE (2007) Melanocyte biology and skin pigmentation. Nature 445:843–850
18. Gupta AK, Gover MD, Nouri K, Taylor S (2006) The treatment of melasma: a review of clinical trials. Am Acad Dermatol 55:1048–1065. https://doi.org/10.1016/j.jaad.2006.02.009
19. Jung JC, Lee JH, Oh S, Lee JG, Park OS (2004) Synthesis and antitumor activity of 4-hydroxycoumarin derivatives. Bioorg Med Chem Lett 14:5527–5531. https://doi.org/10.1016/j.bmcl.2004.09.009
20. Abdelhafez OM, Amin KM, Batran RZ, Maher TJ, Nada SA, Sethumadhavan S (2010) Synthesis, anticoagulant and PIVKA-II induced by new 4-hydroxycoumarin derivatives. Bioorg Med Chem 18:3371–3378. https://doi.org/10.1016/j.bmc.2010.04.009
21. Timonen JM, Nieminen RM, Sareila O, Goulas A, Moilanen LJ, Haukka M, Vainiotalo P, Moilanen E, Aulaskari PH (2011) Synthesis and anti-inflammatory effects of a serie of novel 7-hydroxycoumarin derivatives. Eur J Med Chem 46:3845–3850. https://doi.org/10.1016/j.ejmech.2011.05.052
22. Li J, Hou Z, Li F, Zhang Z, Zhou Y, Luo X, Li M (2014) Synthesis, photoluminescent, antibacterial and theoretical study of 4-hydroxycoumarin derviatives. Mol Str 1075:509–514. https://doi.org/10.1016/j.molstruc.2014.07.010
23. Kurt BZ, Gazioglu I, Sonmez F, Kucukislamoglu M (2015) Synthesis, antioxidant and anticholinesterase activities of novel coumarylthiazole derivatives. Bioorg Chem 59:80–90. https://doi.org/10.1016/j.bioorg.2015.02.002
24. Promden W, Viriyabancha W, Monthakantirat O, Umehara K, Noguchi H, De-Eknamkul W (2018) Correlation between the potency of flavonoids on mushroom tyrosinase inhibitory activity

and melanin synthesis in melanocytes. Molecules 23:1403–1413. https://doi.org/10.3390/molecules23061403

25. Wu L, Liu B, Li Q, Chen J, Tao L, Hu G (2012) Design, synthesis and anti-fibrosis activity study of N1-substituted phenylhydroquinolone derivatives. Molecules 17:1373–1387. https://doi.org/10.3390/molecules17021373

26. Zghab I, Trimeche B, Touboul D (2014) A regioselective 1,3-dipolar cycloaddition for the synthesis of novel spiro-chromenethiadiazole derivatives. C R Chimie 17:171–178. https://doi.org/10.1016/j.crci.2013.08.004

27. Zardi-Bergaoui A, Jelassi A, Daami-Remadi M, Harzallah-Skhiri F, Flamini G, Ascrizzi R, Ben Jannet H (2019) Chemical composition and bioactivities of essential oils from *Pulicaria vulgaris* subsp. *dentata* (Sm.) Batt. growing in Tunisia. J Essent Oil Res, 111–120. https://doi.org/10.1080/10412905.2019.1698468.

28. Aissa I, Nimbarte VD, Zardi-Bergaoui A, Znati M, Flamini G, Ascrizzi R, Ben Jannet H (2019) Isocostic acid, a promising bioactive agent from the essential oil of *Inula viscosa* (L.) :insights from drug likeness properties, molecular docking, and SAR analysis. Chem Biodiversity 16:e1800648. https://doi.org/10.1002/cbdv.201800648.

29. Mo J, Yang H, Chen T, Li Q, Lin H, Feng F, Liu W, Qu W, Guo Q, Chi H, Chen Y, Sun H (2019) Design, synthesis, biological evaluation, and molecular modeling studies of quinoline-ferulic acid hybrids as cholinesterase inhibitors. Bioorg Chem 93:103310. https://doi.org/10.1016/j.bioorg.2019.103310

30. Ismaya WT, Rozeboom HJ, Weij A, Mes JJ, Fusetti F, Wichers HJ, Dijkstra BW (2011) Crystal structure of *Agarius bisporus* Mushroom Tyrosinase: identity of the tetramer subunits and interaction with tropolone. Biochemistry 50:5477–5486. https://doi.org/10.1021/bi200395t

31. Trott O, Olson AJJ (2010) Autodock Vina: improving the speed and accuracy of dockinh with a new scoring function, efficient optimization, and multithreading. Comput Chem 31:455–461. https://doi.org/10.1002/jcc.21334

32. Brus B, Kosa U, Turk S, Pislar A, Coquelle N, Kos J, Stojan J, Colletier JP, Gobec S (2014) Discovery, biological evaluation, and crystal structure of a novel nanomolar selective butyrylcholinesterase inhibitor. J Med Chem 57:8167–8179. https://doi.org/10.1021/jm501195e